Quantifying the daily harvest of fermentation products from the human gut microbiota – Supplementary Figures

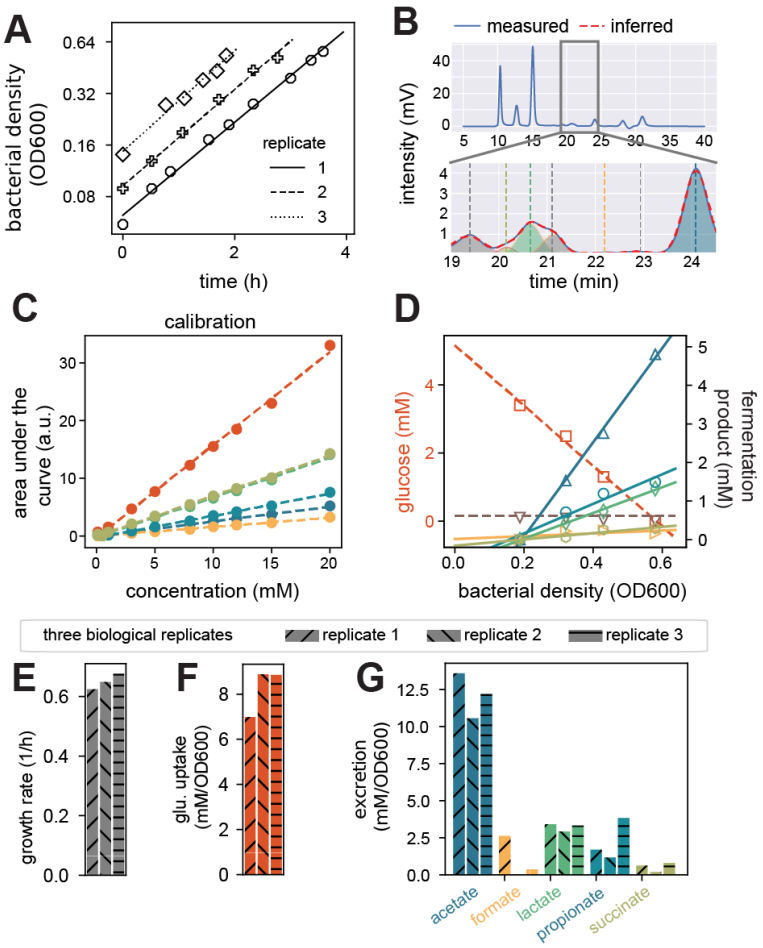

Figure S1. Experimental workflow to determine the per-biomass excretion and consumption rates of metabolites. (A) Optical densities (OD600) were measured over time and samples were taken at different OD600 values during exponential growth (symbols). Culturing in two steps included a pre-culture phase before sample taking to ensure steady growth which promotes the precise determination of uptake and excretion per biomass. Different lines show three independent biological replications. **(B)** These samples were then analyzed for metabolites using HPLC with a refractive index sensor. Peaks for specific metabolites were identified, computationally isolated, and the areas under the curve they cover were quantified using a Python-based data analysis pipeline we have developed. **(C)** Obtained peak areas were then compared to the shown component-specific standard curves to determine their concentrations. **(D)** Linear fits describing the change of these concentrations with optical density, as expected for steady growth, were then used to calculate the per biomass production and consumption of different metabolites. **(E,F)** Per-biomass excretion of FPs, $\{e\_i\}$, and uptake of glucose, u, for three biological replicates. **(G)** Exponential growth rates μ of three biological replicates, obtained by a linear regression on the log-transformed OD data shown in (A). From these numbers excretion and uptake per time can also be calculated. Exemplary data shown here for *B. theta* growing in YCA medium. Similar plots for other species and growth conditions are shown in **Supplementary Dataset 1.**

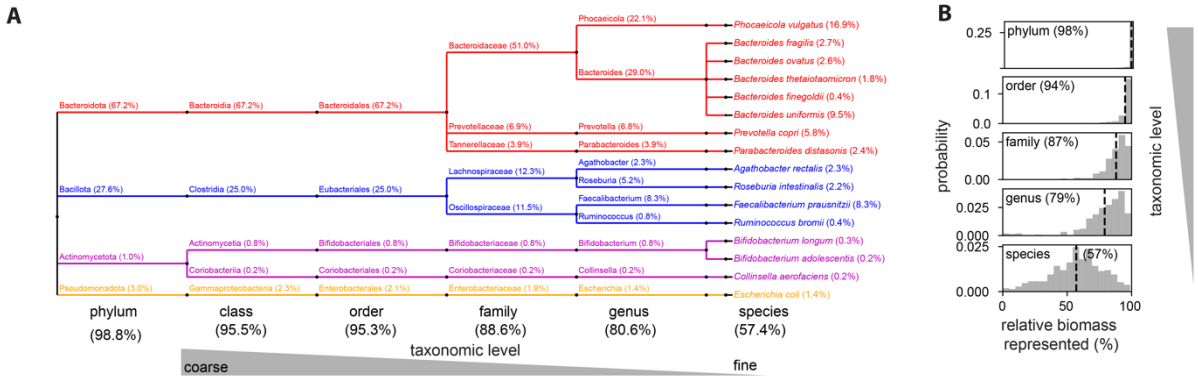

Figure S2. Taxonomic relation and biomass coverage of experimentally characterized strains. (A) Phylogenetic tree of the 16 characterized human gut microbiota strains. Branch labels indicate the names of different taxonomic groups. Numbers show the average coverage these strains represent on the species and higher taxonomic levels in a collection of microbiome samples from healthy individuals. For example, the 16 strains account for 57.4% of all bacterial biomass. **(B)** Breakdown of the sample-to-sample variation of this coverage. Average numbers and distributions for healthy participants presented in (*1*, *2*). Coverage for additional studies is shown in the **Interactive Figure 1**.

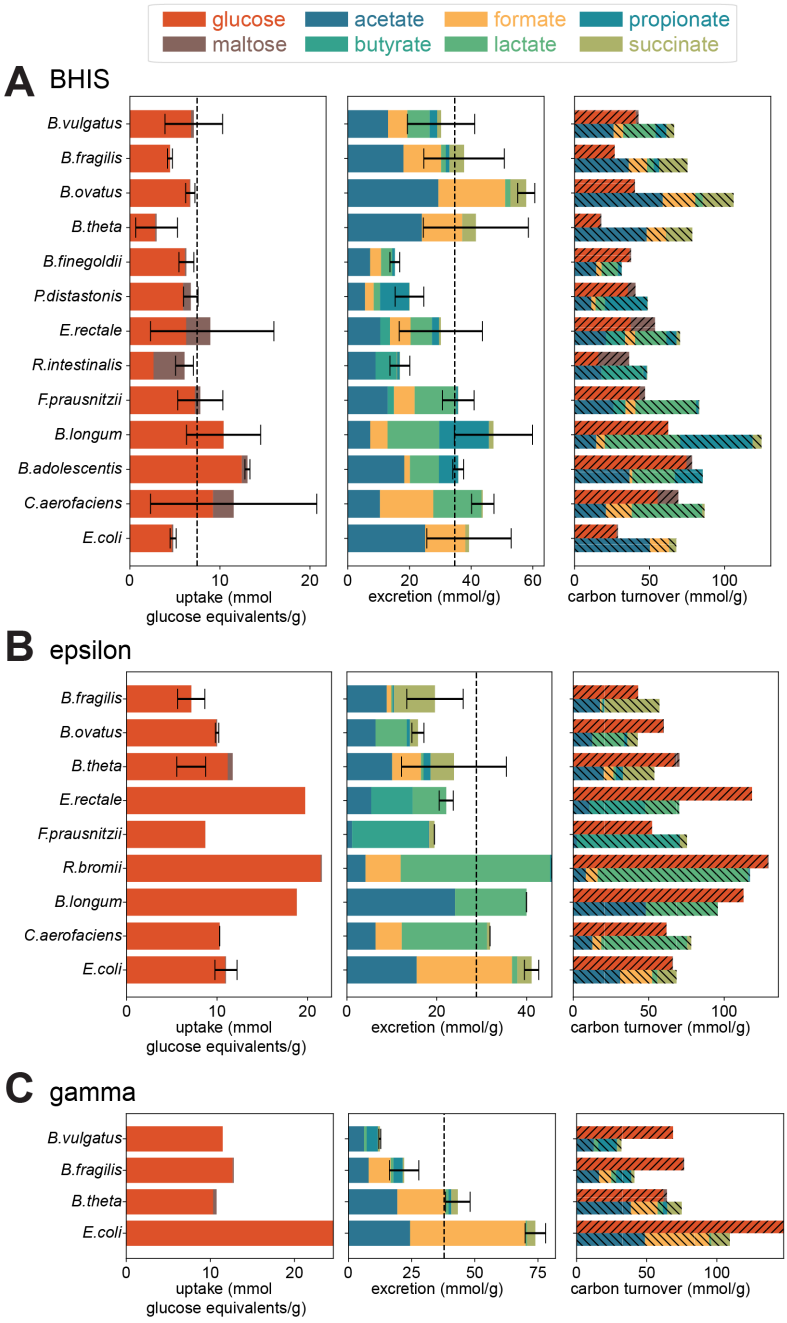

Figure S3. Uptake and excretion characteristics for growth in different media. Sugar uptake and FP excretion per biomass for growth of different gut species in three different media (BHIS, γ, and ϵ). Complexity of medium composition decreases from BHIS (A) to YCA (**Figure 1 D-F**) to epsilon (C) and gamma medium (D). See Methods for details on media composition. With decreasing medium complexity fewer of the sixteen strains can grow.

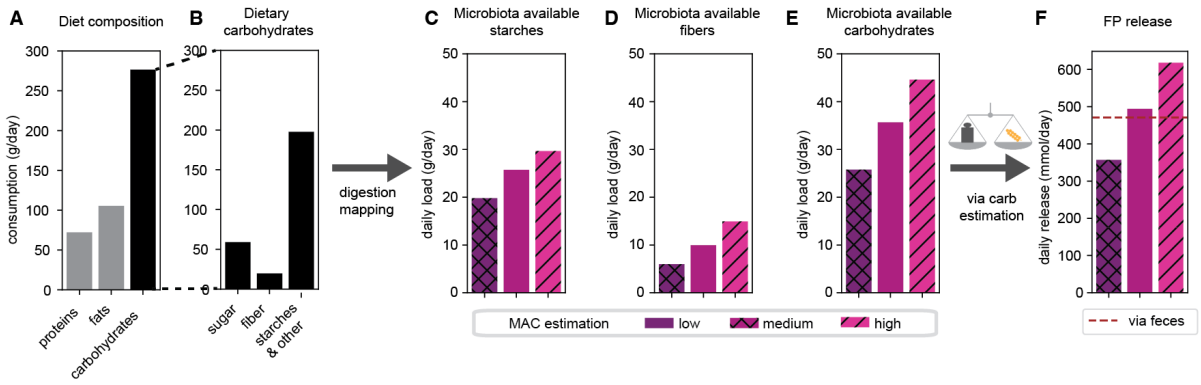

Figure S4. British reference diet – major composition characteristics and variation of the microbiota available carbohydrates with assumptions on complex carbohydrate digestion. (A, B) Diet composition as reported in (*3*). **(C, D, E)** Different mapping assumptions (see **Figure 2I** and **SI Text 4**) lead to varying amounts of microbiota available starches and fibers, the sum of which is the total amount of microbiota available carbohydrates. The medium case corresponds to the data shown in the main text. **(F)** These different assumptions lead to different results when calculating FP release. Parameters used follow typically observed ranges of starch content and fiber digestion, with 15% starch passage and 75% microbial fiber digestion for the high case (poor complex carbohydrate digestion along the upper digestive tract), 13% starch passage and 50% fiber digestion for the medium case, and 10% starch passage and 30% fiber digestion for the low case (efficient complex carbohydrate digestion along the upper digestive tract).

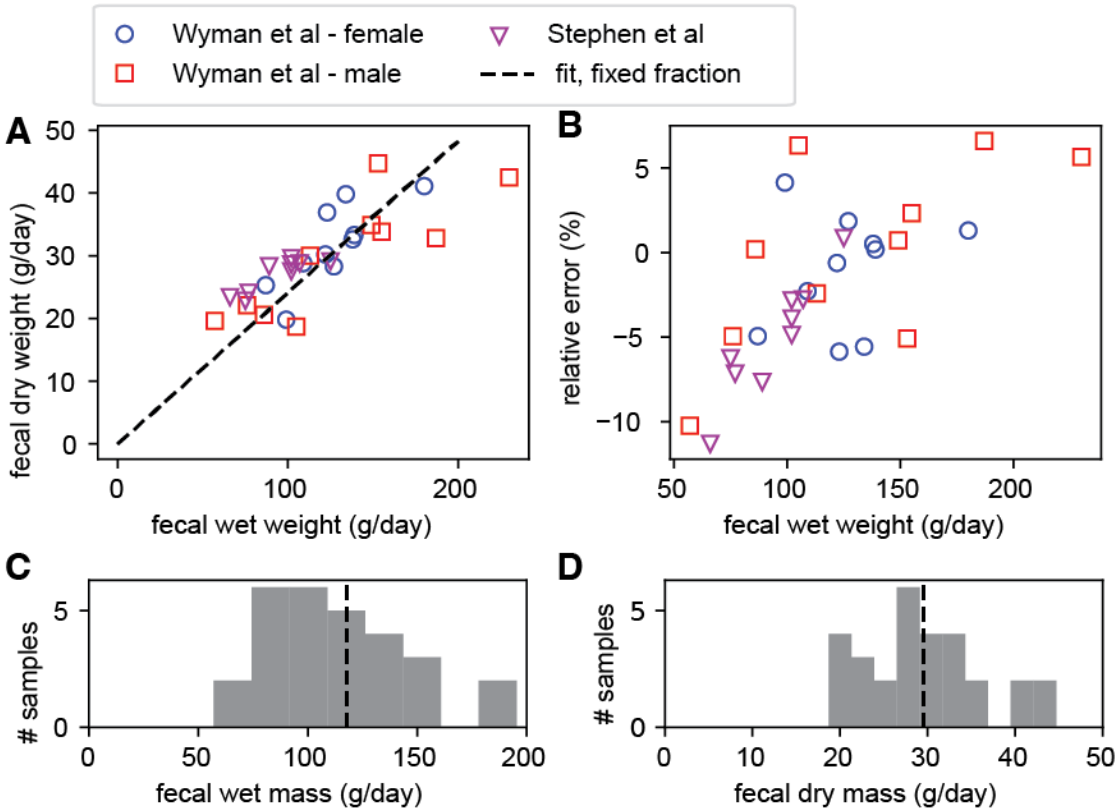

Figure S5. Fecal wet and dry weight for the British reference diet. (A) To describe the relation between fecal dry and wet weight we use data from (*4*) where both values are reported. A linear regression (dashed line) assuming a fixed fraction of dry weight per wet weight describes the relation well. **(B)** Relative error of the linear regression model. Low errors smaller than 10% confirm the linear model. **(C, D)** Histograms of fecal wet and dry weight to illustrate their substantial variation.

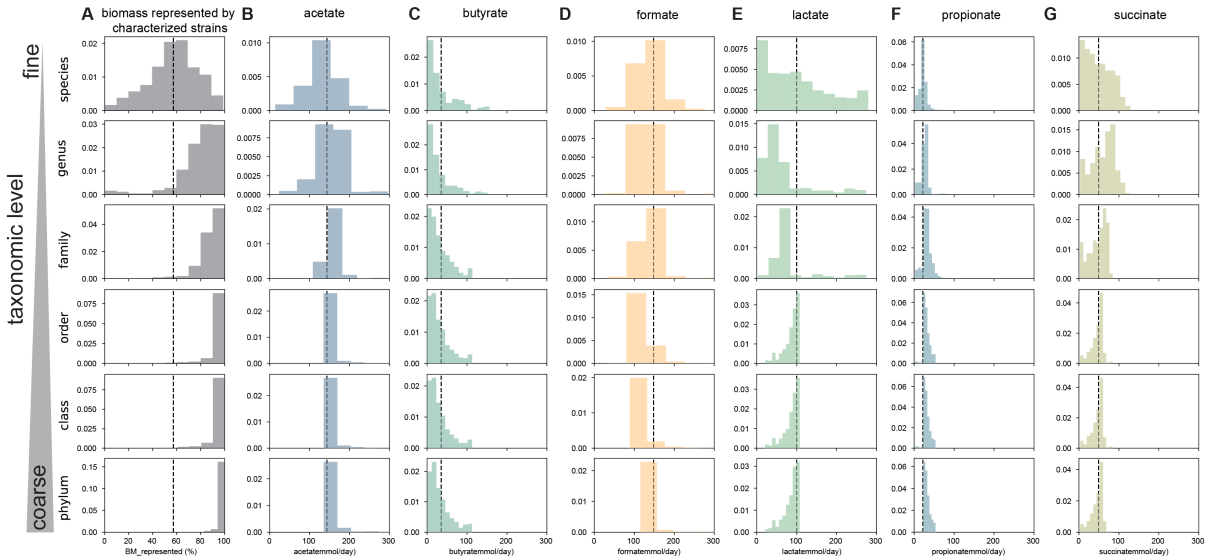

Figure S6. Representation and analysis of fermentation product release on different taxonomic levels. To decide which taxonomic level to use for our analysis, we probed how much of the abundance and metabolic diversity observed in the healthy human gut microbiome (*1*, *2*) we covered with the 16 strains we have characterized experimentally. Covered abundance changed with the taxonomic level we chose for our analysis, with a coarser level leading to higher coverage (grey histograms). For example, on the species level, the characterized strains represent an average of about 60% of microbial biomass, while on the phylum level, they strains represent on average more than 90% of bacterial biomass. Thus, choosing a coarser level will lead to a higher representation by experimentally characterized strains, and we need to make fewer assumptions on how to describe the uptake and excretion rates of unrepresented bacterial biomass. On the other hand, we also lose resolution in describing the production of specific FPs when choosing a taxonomic level that is too coarse. Particularly, the metabolic behaviors of strains belonging to different taxonomic groups might differ substantially at coarser taxonomic levels. For example, consider the production of propionate, which is produced in substantial quantities by some, but not all, species of the phylum Bacteroidota. When using average uptake and excretion rates including all experimentally characterized strains belonging to the Bacteroidota phylum, we will thus use possible differences in propionate release. As the best compromise, we thus chose the family level for our analysis, as biomass coverage is already very high while we avoid too much averaging out of strain-level differences. See **SI Text 6** for further discussion.

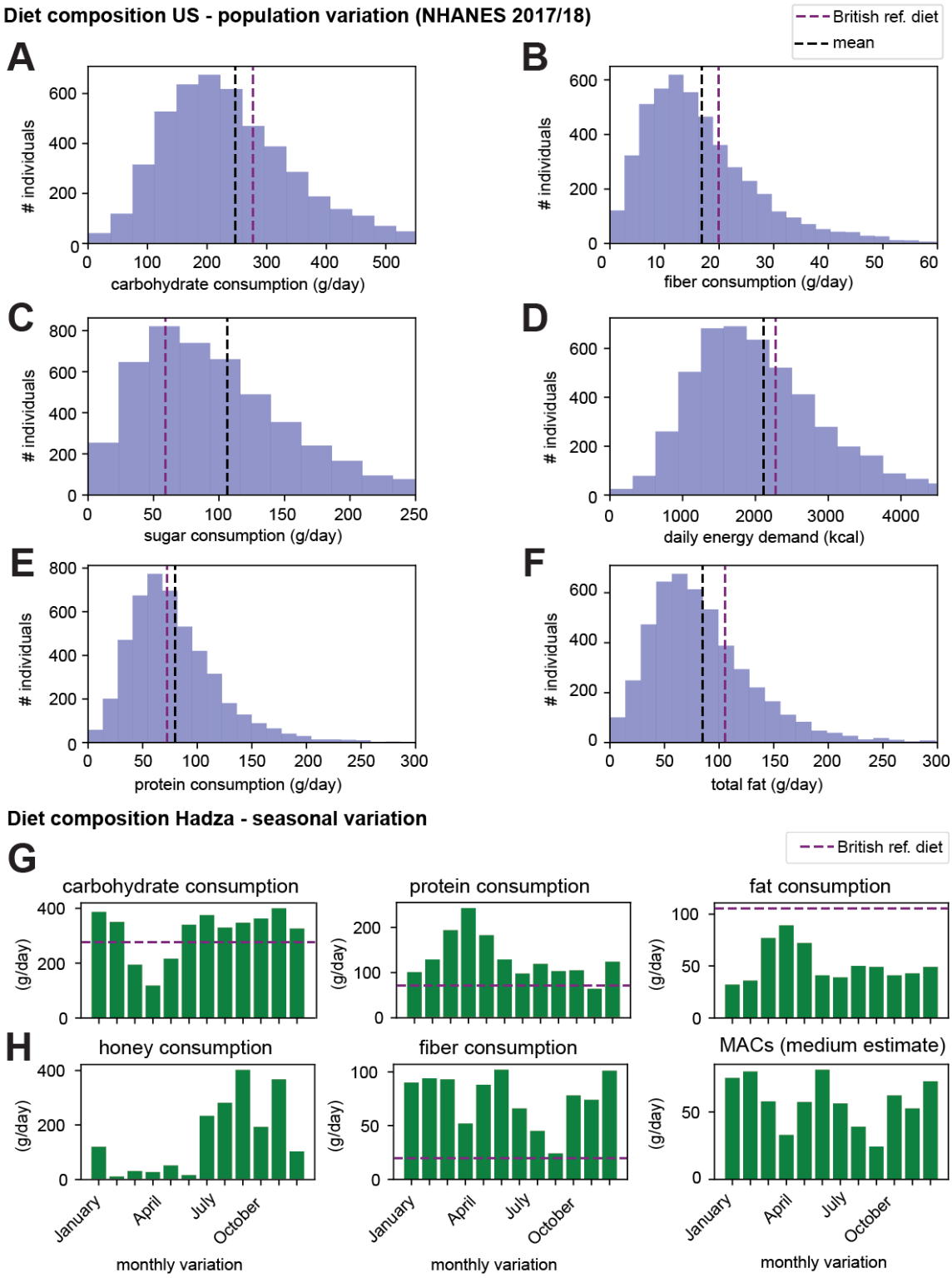

Figure S7. Major dietary characteristics for the US population and the Hadza. Data underlying the estimates for microbiota available carbohydrates and total FP production shown in Figure 3. **(A-F)** Distribution of different dietary characteristics across the NHANES 2017/2018 cohort (*5*). Black dashed lines indicate means of distributions. **(G,H)** Per-capita breakdown of major diet components based on food collected by a group of Hadza people, as reported by Pontzer and Wood (*6*). Purple dashed lines in different panels indicate corresponding numbers for the British reference diet (**Figure S4**).

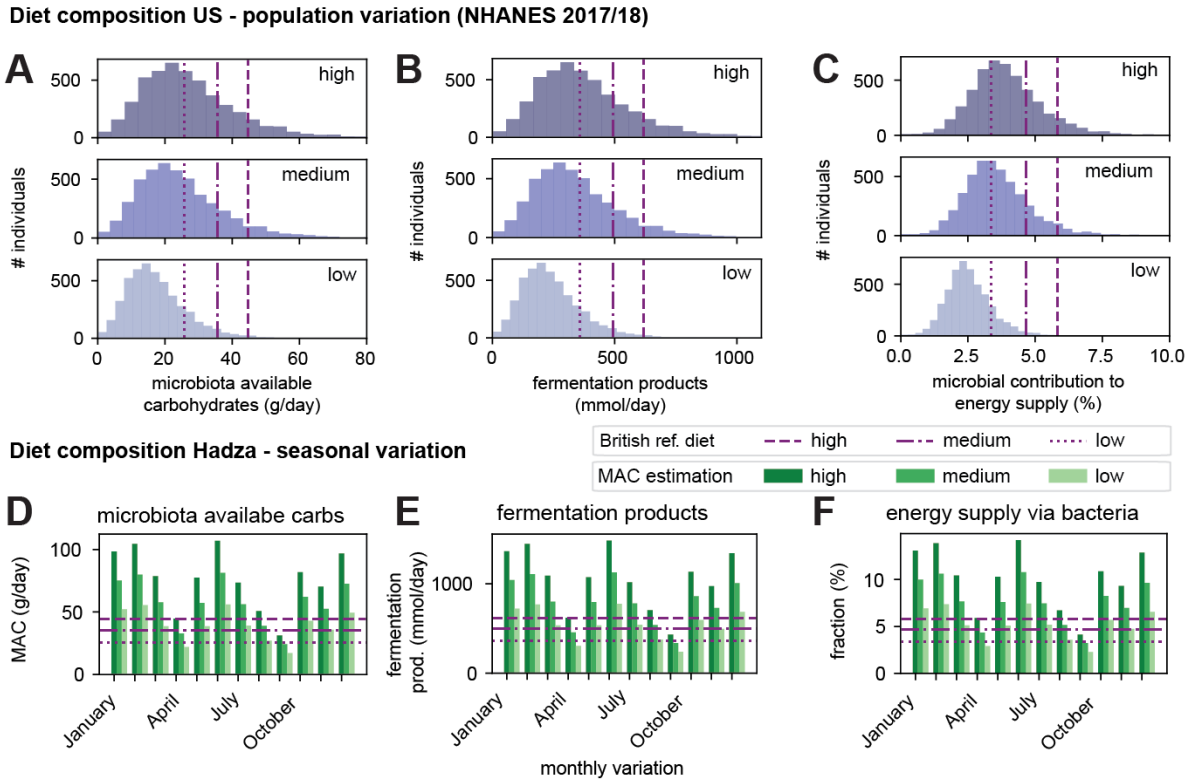

Figure S8. Variation of fermentation product release with diet, given different assumptions of carbohydrate digestion. We analyzed the change in microbiota available carbohydrate in different diets to estimate the total FP release (**Figure 4 A,B**), when changing the assumptions on carbohydrate degradation along the upper digesting tract within observed ranges (see **Figure 2I**, **Figure S4**, **SI Text 4** for further discussion of the mapping). **(A-C)** Changes in microbiota available carbohydrate, total FP release, and microbial contribution to the daily energy demand with reported variations in carbohydrate consumption reported for the NHANES 2017/2018 cohort. **(D-F)** Changes in microbiota available carbohydrates, total FP release, and microbial contribution to the daily energy demand with the reported month-to-month variation of per-person carbohydrate amount in food in a group of Hadza people. As in **Figure S4**, and following observations for the British reference scenario (*7*), parameters used to describe the mapping between consumed and microbiota available carbohydrates are 15% starch passage and 75% fiber digestion for the high case, 13% starch passage and 50% fiber digestion for the medium case, and 10% starch passage and 30% fiber digestion for the low case. In the main text, data for the standard mapping are shown. Purple lines indicate corresponding estimations for the British reference diet.

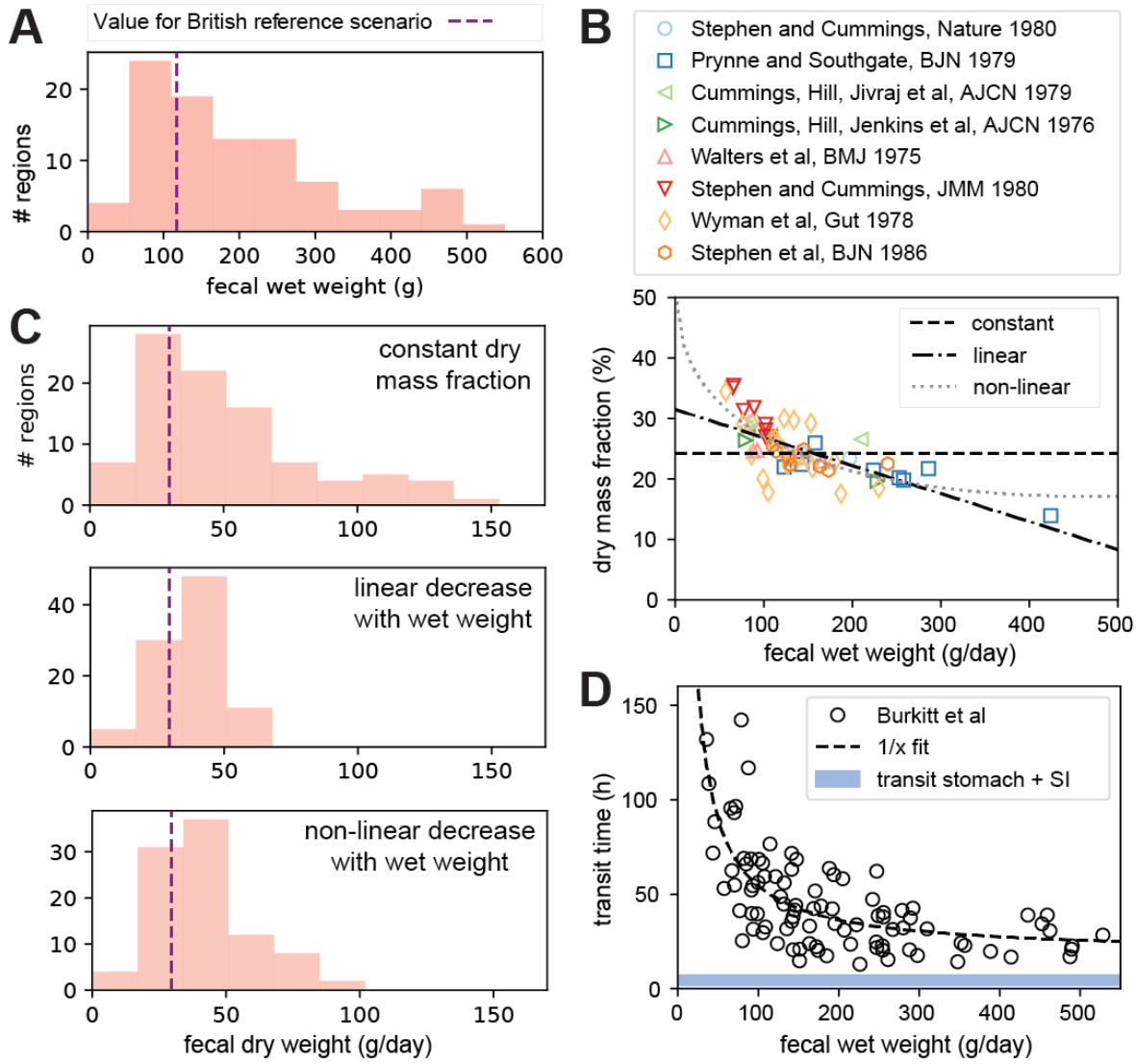

Figure S9. Global variation in fecal weight and variation of fermentation product release with fecal water content. (A) Variation in fecal wet weight in humans of various backgrounds and lifestyles, as reported in (*8*). **(B)** Shown data (markers) were collected from different studies that measured fecal wet and dry weight for different cohorts and dietary compositions (*4*, *9*–*15*). When the variation in fecal output gets larger, water content in feces increases. Therefore, the assumption of a constant ratio of dry weight per wet weight we have been using for the British reference case (**Figure S5**) leads to substantial errors in describing the observations ("constant", dashed line). To account for larger variations in water content, we formulated two additional models to fit the data. In the linear model, the dry mass fraction (α_{dw}) decreases linearly with fecal wet weight ("linear", dotted dashed line, $\alpha_{dw} = 1 - 4.63 * M_{feces,wet} + 0.69$). In the non-linear model, the dry mass fraction (α_{dw}) decreases approximately linearly with fecal wet weight when wet weight is low, but it hardly changes anymore when fecal wet weight is high ("non-linear", dotted line, $\alpha_{dw} = 1 - (0.49 + 0.03 \cdot 1/\sqrt{g} * \sqrt{M_{feces,wet}} - 0.0007 * M_{feces,wet} \cdot 1/g)$. Both models describe the trends of the available data well. We expect the dry mass content to decrease further with higher fecal wet weight as very high weights are likely caused by a higher water content bound to fibers in feces. However, as no parallel measurements of fecal dry and wet weights are available for

very high weights, the non-linear model provides a well-supported upper bound of fecal dry weight. **(C)** With these different models, we then estimated the fecal dry weight for the data reported in (*8*). Notably, the variation in fecal dry weight decreases substantially when accounting for the adjustment in dry mass fraction. For the estimations discussed in the main text, we used the non-linear model. As such, these numbers provide an upper bound estimate. **(D)** The transit time (i.e., the time it takes for ingested material to pass the entire digestive tract), decreases with fecal wet weight, described well by an inversely proportional relation (dashed line, $\tau_{transit} \sim \frac{1}{M_{feces,wet}}$). Data re-plotted from Burkitt et al. (*8*). As transit through the stomach and small intestine is relatively short (highlighted in blue), this strong variation in transit time is primarily due to changes in the time biomass remains within the large intestine. Notably, the substantial variation of this time can impact the efficiency with which the microbiota digests complex carbohydrates along the large intestine. Particularly when fecal wet weight is high and transit times are short, the microbiota might simply not have enough time to complete digestion, and a higher fraction of complex carbohydrates end up undigested in feces. As such, and similar to the estimation of fecal dry weight, our estimations are again an upper bound for the daily production of fermentation products, particularly when fecal wet weights are large.

References – Supplementary Figures

1. J. Lloyd-Price, C. Arze, A. N. Ananthakrishnan, M. Schirmer, J. Avila-Pacheco, T. W. Poon, E. Andrews, N. J. Ajami, K. S. Bonham, C. J. Brislawn, D. Casero, H. Courtney, A. Gonzalez, T. G. Graeber, A. B. Hall, K. Lake, C. J. Landers, H. Mallick, D. R. Plichta, M. Prasad, G. Rahnavard, J. Sauk, D. Shungin, Y. Vázquez-Baeza, R. A. White, J. Braun, L. A. Denson, J. K. Jansson, R. Knight, S. Kugathasan, D. P. B. McGovern, J. F. Petrosino, T. S. Stappenbeck, H. S. Winter, C. B. Clish, E. A. Franzosa, H. Vlamakis, R. J. Xavier, C. Huttenhower, Multi-omics of the gut microbial ecosystem in inflammatory bowel diseases. *Nature* **569**, 655–662 (2019).

2. M. Schirmer, E. A. Franzosa, J. Lloyd-Price, L. J. McIver, R. Schwager, T. W. Poon, A. N. Ananthakrishnan, E. Andrews, G. Barron, K. Lake, M. Prasad, J. Sauk, B. Stevens, R. G. Wilson, J. Braun, L. A. Denson, S. Kugathasan, D. P. B. McGovern, H. Vlamakis, R. J. Xavier, C. Huttenhower, Dynamics of metatranscription in the inflammatory bowel disease gut microbiome. *Nat. Microbiol.* **3**, 337–346 (2018).

3. *Household Food Consumption and Expenditure: Annual Report of the National Food Survey Committee* (H.M.S.O., ed. 1976) (1976).

4. J. B. Wyman, K. W. Heaton, A. P. Manning, A. C. Wicks, Variability of colonic function in healthy subjects. *Gut* **19**, 146–150 (1978).

5. *National Health and Nutrition Examination Survey (NHANES) Data 2017-2018* (Centers for Disease Control and Prevention (CDC). National Center for Health Statistics (NCHS), Hyattsville, MD: US Department of Health and Human Services) (2018).

6. H. Pontzer, B. M. Wood, Effects of Evolution, Ecology, and Economy on Human Diet: Insights from Hunter-Gatherers and Other Small-Scale Societies. *Annu. Rev. Nutr.* **41**, 363–385 (2021).

7. K. N. Englyst, S. Liu, H. N. Englyst, Nutritional characterization and measurement of dietary carbohydrates. *Eur. J. Clin. Nutr.* **61**, S19–S39 (2007).

8. D. P. Burkitt, A. R. P. Walker, N. S. Painter, Effect of Dietary Fibre on Stools and Transit-Times, and its Role in the Causation of Disease. *The Lancet* **300**, 1408–1411 (1972).

9. J. H. Cummings, M. J. Hill, D. J. Jenkins, J. R. Pearson, H. S. Wiggins, Changes in fecal composition and colonic function due to cereal fiber. *Am. J. Clin. Nutr.* **29**, 1468–1473 (1976).

10. A. M. Stephen, J. H. Cummings, The Microbial Contribution to Human Fecal Mass. *J. Med. Microbiol.* **13**, 45–56 (1980).

11. A. M. Stephen, J. H. Cummings, Mechanism of action of dietary fibre in the human colon. *Nature* **284**, 283–284 (1980).

12. C. J. Prynne, D. A. T. Southgate, The effects of a supplement of dietary fibre on faecal excretion by human subjects. *Br. J. Nutr.* **41**, 495–503 (1979).

13. J. H. Cummings, M. J. Hill, T. Jivraj, H. Houston, W. J. Branch, D. J. A. Jenkins, The effect of meat protein and dietary fiber on colonic function and metabolism I. Changes in bowel habit, bile acid excretion, and calcium absorption. *Am. J. Clin. Nutr.* **32**, 2086–2093 (1979).

14. R. L. Walters, I. M. Baird, P. S. Davies, M. J. Hill, B. S. Drasar, D. A. Southgate, J. Green, B. Morgan, Effects of two types of dietary fibre on faecal steroid and lipid excretion. *BMJ* **2**, 536–538 (1975).

15. A. M. Stephen, H. S. Wiggins, H. N. Englyst, T. J. Cole, B. J. Wayman, J. H. Cummings, The effect of age, sex and level of intake of dietary fibre from wheat on large-bowel function in thirty healthy subjects. *Br. J. Nutr.* **56**, 349–361 (1986).

Quantifying the daily harvest of fermentation products from the human gut microbiota – Supplementary Tables and Text

Markus Arnoldini[1#], Richa Sharma[2,*], Claudia Moresi[1,*], Griffin Chure[2], Julien Chabbey[1], Emma Slack[1], Jonas Cremer[2#]

[1] Department of Health Science and Technology, ETH Zürich, Zürich, Switzerland
[2] Department of Biology, Stanford University, Stanford CA, USA
* Contributed equally
# markus.arnoldini@hest.ethz.ch, jbcremer@stanford.edu

SUPPLEMENTARY TABLES

Table S1: Bacterial strains. We quantified yields and FP excretion for the following gut strains. In the table, the updated phylum classification system is used. The old names for Bacteroidota, Bacillota, Actinomycetota, and Pseudomonadota were Bacteroidetes, Firmicutes, Actinobacteria, and Proteobacteria, respectively.

Species	Phylum	Class	Order	Family	Strain ID	source
Phocaeicola vulgatus (formerly *Bacteroides vulgatus*)	Bacteroidota	Bacteroidia	Bacteroidales	Bacteroidaceae	DSM 1447	DSMZ
Bacteroides fragilis	Bacteroidota	Bacteroidia	Bacteroidales	Bacteroidaceae	ATCC 25285	ATCC
Bacteroides ovatus	Bacteroidota	Bacteroidia	Bacteroidales	Bacteroidaceae	ATCC 8483	ATCC
Bacteroides thetaiotaomicron	Bacteroidota	Bacteroidia	Bacteroidales	Bacteroidaceae	ATCC 29148	ATCC
Bacteroides finegoldii	Bacteroidota	Bacteroidia	Bacteroidales	Bacteroidaceae	H-727	BEI resources
Bacteroides uniformis	Bacteroidota	Bacteroidia	Bacteroidales	Bacteroidaceae	ATCC 8492	ATCC
Parabacteroides distasonis	Baceroidota	Bacteroidia	Bacteroidales	Bacteroidaceae	H-169	BEI resources
Prevotella copri	Bacteroidota	Bacteroidia	Bacteroidales	Prevotellaceae	DSM 18205	DSMZ
Agathobacterium rectalis (formerly	Bacillota	Clostridia	Eubacteriales	Lachnospiraceae	ATCC 33656	ATCC

Eubacterium rectale)						
Faecalibacterium prausnitzii	Bacillota	Clostridia	Eubacteriales	Oscillospiraceae	DSM 17677	DSMZ
Roseburia intestinalis	Bacillota	Clostridia	Eubacteriales	Lachnospiraceae	DSM 14610	DSMZ
Ruminococcus bromii	Bacillota	Clostridia	Eubacteriales	Osciollospiraceae	ATCC 27255	ATCC
Bifidobacterium adolescentis	Actinomycetota	Actinomycetia	Bifidobacteriales	Bifidobacteriaceae	DSM 20083	DSMZ
Bifidobacterium longum	Actinomycetota	Actinomycetia	Bifidobacteriales	Bifidobacteriaceae	DSM 20219	DSMZ
Collinsella aerofaciens	Actinomycetota	Coriobacteriia	Coriobacteriales	Coriobacteriaceae	DSM 3979	DSMZ
Escherichia coli	Pseudomonadota	Gammaproteobacteria	Enterobacterales	Enterobacteriaceae	NCM 3722	(*1*)

Table S2. Per biomass uptake and FP excretion. Based on in-vitro measurements of all 16 strains as outlined in **SI Text 2 and Figure S1**. Data for growth in YCA medium. Unweighted averages and range observed across all strains.

Observable	**Symbol**	**Species average**	**Cross-species range**	**Unit**
Carbohydrate uptake	u_{carbs}	11.7	$6.1 - 16.7$	$mmol\ glucose\ equivalents\ /g$
Total excretion	e_{tot}	29.1	$8.0 - 19.1$	$mmol/g$
Acetic acid excretion	e_{act}	11.2	$0.1 - 27.2$	$mmol/g$
Butyric acid excretion	e_{but}	1.5	$0.0 - 8.7$	$mmol/g$
Formic acid excretion	e_{for}	7.4	$1.8 - 20.2$	$mmol/g$
Lactic acid excretion	e_{lac}	4.7	$0.0 - 24.1$	$mmol/g$
Propionic acid excretion	e_{pro}	2.1	$0.1 - 5.8$	$mmol/g$
Succinic acid excretion	e_{suc}	2.2	$0.0 - 7.1$	$mmol/g$

Table S3: Major observables used in estimation for British Reference Scenario.
*variation based on observed variation reported in (*2*)
**variation based on reported variation in (*3*)

Observable	Symbol	Value	Reference
Fecal wet weight	$M_{feces,wet}$	$118g$	(*2*, *4*)
Fraction dry mass	α_{dw}	0.25	(*2*, *4*), see Figure S5
Fecal dry weight*	$M_{feces,dry}$	$29.5 \pm 6.8\ g$	this study
Fraction of bacterial dry mass per fecal dry mass	α_{bact}	0.55	(*4*)
Microbiota-available carbohydrates (standard estimation)**	M_{Carb}	$35.7 \pm 9\ g$	(*3*)

Table S4. Properties of fermentation products.
* Enthalpy values based on (*5*)
** we do not include formic acid when estimating the FP contribution to host energy demand

Fermentation product	Molecular weight (g/mol)	Carbon atoms per molecule	Combustion enthalpy H_i (kJ/mol)*
Acetic acid	60.05	2	0.88
Butyric acid	88.11	4	2.18
Formic acid**	46.03	1	0.26
Lactic acid	90.08	3	1.38
Propionic acid	74.08	3	1.55
Succinic acid	118.09	4	1.51

Table S5. List of media components, chemicals, and laboratory equipment used.

Item	Use	Supplier	Item number

Brain Heart Infusion	media component	Thermo Fisher Diagnostics	CM1135B
Hemin	media component	Sigma Aldrich	H9039-1G
L-Cysteine	media component	Sigma Aldrich	168149-25G
Casitone	media component	BD Biosciences	225930
Yeast Extract	media component	Thermo Fisher Diagnostics	LP0021B
Meat Extract	media component	Sigma Aldrich	70164-100G
K2HPO4	media component	Carl Roth	P749.2
KH2PO4	media component	Sigma Aldrich	60220-1KG
NaCl	media component	Sigma Aldrich	71380-1KG
D-(+)-Glucose monohydrate	media component	Millipore	49159-1KG
D-(+)-Maltose monohydrate	media component	Sigma Aldrich	M5885-100G
CaCl2 dihydrate	media component	Sigma Aldrich	31307-1KG
MgCl2 hexahydrate	media component	Sigma Aldrich	63065-1KG
MnCl2 tetrahydrate	media component	Sigma Aldrich	M8054-100G
CoCl2 hexahydrate	media component	Sigma Aldrich	C8661-25G
FeSO4 hydrate	media component	Sigma Aldrich	307718-100G
NaHCO3	media component	Sigma Aldrich	S5761
NH4Cl	media component	Sigma Aldrich	31107-1KG
Menadione	media component	Sigma Aldrich	M5625-25G
Folinic Acid	media component	Sigma Aldrich	47612-250MG
Cobalamine (Vitamin B12)	media component	Sigma Aldrich	V6629-250MG
Sodium Acetate	media component/ HPLC standard	Sigma Aldrich	1.06268.0250

BME vitamins 100x solution	media component	Sigma Aldrich	B6891-100ML
Tryptone	media component	Thermo Fisher Diagnostics	LP0042B
0.1M H2SO4 in water for ion chromatography	HPLC mobile phase	Sigma Aldrich	68279-1L
Sodium Butyrate	HPLC standard	Sigma Aldrich	303410-100G
Sodium Propionate	HPLC standard	Sigma Aldrich	P1880-100G
Sodium DL-Lactate	HPLC standard	Sigma Aldrich	71720-25G
Sodium Succinate dibasic hexahydrate	HPLC standard	Sigma Aldrich	S9637-100G
Sodium formate	HPLC standard	Sigma Aldrich	71539-500G
Glass culture tubes	laboratory material		
Anaerobic workbench	laboratory material	Coy Labs	Anaerobic Chamber Type A, Vinyl
Shaking dry bath	laboratory material	Eppendorf	ThermoMixer C
Quartz semi-micro cuvette	laboratory material	VWR	634-9081
Spectrophotometer	laboratory material	Thermo Scientific	Lambda/Genesys30
Corning Costar Spin-X centrifuge filter tubes, sterile	laboratory material	Sigma Aldrich	CLS8160-96EA
HPLC machine	measure FPs and sugars	Thermo Scientific/Shimadzu	Ultimate 3000/Prominence LC2030C
Phenomenex Rezex ROA H+ (8%), 300 x 7.8mm	HPLC column	Phenomenex	00H-0138-K0

SUPPLEMENTARY TEXT

Section 1: Anaerobic growth is constrained by balancing ATP generation and redox balance

Bacteria growing in anoxic conditions face a threefold challenge: they need to generate sufficient energy, retain enough carbon to produce biomass, and keep their redox state in balance (*6*). In this section, we briefly summarize the biochemical origin of this challenge for gut bacteria. To survive and grow, bacteria have to extract energy and building blocks for biomass synthesis from nutrients available in their environments. Under anoxic conditions, bacteria also need to find a suitable terminal electron acceptor instead of oxygen, making anaerobic metabolism much less energy efficient than aerobic growth in the presence of oxygen. Biochemically this emerges from the fact that most energy-providing metabolic reactions are redox processes. The electron-donating and electron-accepting parts of these reactions are typically separated and coupled by electron carriers (often nicotinamide adenine dinucleotides, NAD). The donating reaction transfers electrons to the carrier, the accepting reaction transfers electrons from the carrier to an accepting molecule, and both reactions can be coupled with the generation of ATP. Importantly, cells need to balance their redox state, for which every electron-donating reaction needs to be coupled with an electron-accepting reaction. Most obligate anaerobes within the gut use metabolic intermediates as terminal electron acceptors, which are then secreted as fermentation products. These compounds, typically small organic molecules, contain carbon extracted from nutrients that therefore cannot be used to gain more energy or build biomass.

In the large intestine, the main carbon source that is available to the microbiota are carbohydrates that are undigestible by host enzymes. They get metabolized to pyruvate via glycolysis or similar pathways and are then funneled into a limited set of pathways leading to the final fermentation products (**Figure 1A**). Not all bacterial species carry all these pathways, and every given bacterial strain faces the optimization problem discussed above: maximizing growth and survival while keeping its metabolism, including ATP concentrations and redox states, in homeostasis. Importantly, however, these pathways are part of central carbon metabolism, and even though there is variation between species and even between strains of the same species in pathway utilization, the metabolic abilities are typically conserved within genera and often families (see e.g. (*7*, *8*) for *Bacteroides* strains, (*9*, *10*) for analyses of the phylogenetic distribution of propionate production pathways, (*10*–*12*) for analyses of the phylogenetic distribution of butyrate production pathways). We have analyzed how the choice of taxonomic level influences our results (details can be found in the legend to **Figure S6**) and chose the family level as taxonomic level discussed in the main text.

In the following, we summarize the most abundant fermentative pathways that are found in gut bacteria from the different families briefly discuss their limitations. Importantly, the shown net reactions are one possible outcome that preserves stoichiometry, but other combinations are possible.

Bacteroidetes (simplified, (*13*–*15*)): this combination of pathways is typical for in members of the Bacteroidaceae family, represented by *P. vulgatus*, *B. fragilis*, *B. ovatus*, *B. thetaiotaomicron*, *B. finegoldii*, *B. uniformis* in our dataset. Prevotellaceae (represented by *P. copri*) have very similar pathways, but lack the last step for propionate formation and secrete succinate instead (*16*). Also members of the Bacteroidaceae family often skip this last step of the propionate formation pathway and secrete succinate, which has been suggested to be subject to regulation (*17*).

1. 1 Glucose + 2 NAD^+ → 2 Phospoenolpyruvate (PEP) + 2 NADH
2. 2 PEP + 3 ADP + 2NADH → 1 Pyruvate + 1 Propionate (or Succinate) + 3 ATP + 2 NAD^+
3. 1 Pyruvate + 1 ADP → 1 Acetate + 1 ATP

(4. 1 Pyruvate + NADH → 1 Lactate + 1NAD^+)
(5. 1 Pyruvate → 1 Formate)

Net reaction: 1 Glucose + 4 ADP → 1 Propionate + 1 Acetate + 4 ATP

Clostridia (simplified, (*11*, *13*, *18*)): this combination of pathways is typical for gut dwelling members of the class Clostridia, represented by *A. rectalis*, *R. intestinalis*, and *F. prausnitzii* in our dataset. In addition to the stoichiometry below, there is evidence for lactate and acetate cross-feeding into acetyl-CoA and butyrate in *A. rectalis* (*19*).

1. 1 Glucose + 2 NAD+ + 2 ADP → 2 Pyruvate + 2 NADH + 2 ATP

2a. 1 Pyruvate + 1 NADH → 1 Lactate + 1 NAD^+

2b. 1 Pyruvate + 1 ADP → 1 Acetate + 1 ATP

3. 1 Acetate + 1 ATP + 1 CoA → 1 Acetyl-CoA + ADP
4. 1 Acetate + 1 NADH + 1 ADP + 1 Acetyl-CoA → 1 Butyrate + 1 ATP + 1 NAD^+

Net reaction: 1 glucose + 1 ADP → 1 Lactate + 1/2 Butyrate + 1 ATP

Bifidobacteria (*20*): this pathway is characteristic for members of the genus Bifidobacterium, represented by *B. adolescentis* and *B. longum* in our dataset.

1. 2 Glucose + 1 ADP → 2 Xylulose-5-P + 1 Acetate + ATP
2. 2 X-5-P + 6 ADP + 2 NAD+ → 2 Acetate + 2 ATP + 2 Pyruvate + 4 ATP + 2 NADH
3. 2 Pyruvate + 2 NADH → 1 Lactate + 1 NAD+ + 1 Formate + 0.5 Acetate + 0.5 ATP + 0.5 Ethanol + NAD^+

Net reaction: 2 glucose + 7.5 ADP → 3.5 acetate + 0.5 ethanol + 1 lactate + 1 formate + 7.5 ATP

Mixed acid fermentation (*21*): this combination of pathways is used by members of the Enterobacteriaceae family such as *Escherichia coli* and *Salmonella enterica* when growing in anaerobic conditions. In our dataset it is represented by *E. coli*. Ethanol, acteone, butanediol and butyrate have also been shown to be possible fermentation products, which we do not observe in our measurements.

1. 2 Glucose + 4 NAD+ + 4 ADP → 4 Pyruvate + 4 NADH + 4 ATP
2. 1 Pyruvate + 1 ADP → 1 Acetate + 1 ATP
3. 1 Pyruvate + 1 NADH → 1 Lactate + 1 NAD^+
4. 1 Pyruvate + 1 ATP + 2 NADH → 1 Succinate (or 1 Propionate) + 1 ADP + 2 NAD^+

(5. 1 Pyruvate → 1 Formate)

Net reaction: 2 Glucose + 6 ADP + 4 NADH → 1 Acetate + 2 Lactate + 1 Succinate + 6 ATP + 4 NAD^+

For completion, we note that, in addition to substrate level phosphorylation, anaerobic respiration can allow anaerobes to harvest energy from reactions that are insufficiently exergonic to produce ATP, e.g. via the formation of a chemiosmotic gradient coupled to an ATPase analogous to aerobic respiration. In the listing above, we did not include this possibility. However, in the phenomenological data shown in Figure 1, where we measure actual physiological parameters experimentally, we expect both classical fermentation and anaerobic respiration to be involved.

Section 2 - Uptake and excretion measurements

To estimate the daily amount of FP products released by the gut microbiota we experimentally characterized $N_{sp} = 16$ highly abundant species. Following the experimental workflow described in **Figure S1**, we characterized for each species j:

i. the molar amount of carbohydrates bacterial cells consume to support a given amount of bacterial biomass $\{u_j\}$. We denote this as the *per biomass uptake* and it follows from the sum of the experimentally determined glucose and maltose uptake ($u_j = u_{gluc,osej} + 2u_{maltose,j}$ with glucose equivalents as unit) The inverse of this value is commonly also denoted as yield coefficient ($Y_j = 1/u_j$).

ii. the excretion of major fermentation products per bacterial biomass, $\{e_{ij}\}$ with i={acetate, butyrate, formate, lactate, succinate, propionate} denoting the major fermentation products released.

The variation of these numbers across strains is summarized in **Figure 1** and all values are listed in the data tables on the GitHub repository. To derive from these numbers the total daily uptake and FP production in a microbiota sample we need to calculate the cross-species average of the excretion and uptake rates depending on the relative abundance of different strains in a microbiota sample. Specifically, we can calculate the average uptake and excretion rates depending on the average abundance of all experientially characterized species. For example, if *B. uniformis* is the most abundant species in a sample we should also give the measured excretion behavior of this strain a higher weight when determining average excretion rates This approach is introduced in more detail in **SI Text 6** below and we use it to analyze the variation in fermentation product excretion across different microbiota samples (**Figure 3**). However, as a good approximation to consider the daily release of fermentation products, we can also take the simple average we obtain from all characterized strains.

$$u = 1/N_{Sp} \sum_j u_j$$

$$e_i = 1/N_{Sp} \sum_j \epsilon_{jj}$$

These numbers are shown in **Table S2**. To confirm that it is indeed reasonable to work with these average numbers we compared them with the detailed calculation when accounting for the actual

composition of the microbiota. The comparison, shown in the **SI Text Figure 1** below, specifically for microbiota samples from healthy donors, shows only very small differences. Notably, these differences are small here because we characterized highly abundant gut strains which account for most of bacterial biomass across samples.

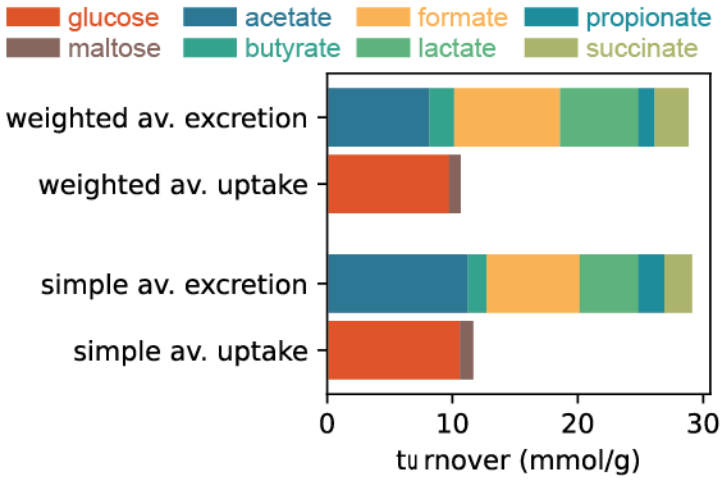

SI Text Figure 1. Using simple average values for excretion and consumption rates gives very similar overall values to weighted averages. Weighing data are microbiota compositions from healthy donors in (*22*, *23*). Determination of average rates as described in **SI Text 6**.

Section 3 Calculation of fermentation product release

In this section, we introduce detailed calculations to estimate the daily release of fermentation products. The corresponding numbers for the British reference scenario are shown in **Table S3**.

Section 3.1 Estimation via feces

The starting point for this estimation is the daily amount of fecal wet weight secreted, $M_{feces,wet}$. With the fraction of fecal dry mass per wet mass, α_{dw}, the daily amount of fecal dry weight excreted follows as

$$M_{feces,dry} = \alpha_{dw} \cdot M_{feces,wet}$$

Given the fraction of bacterial biomass per fecal dry mass, α_{bact}, the daily amount of bacterial dry mass released then follows as

$$M_{feces,bact} = \alpha_{bact} \cdot M_{feces,dry}$$

The total daily amount of fermentation products released to support the growth of this biomass follows as

$$FP_{tot} = \sum_i FP_i = \sum_i e_i M_{feces,bact}$$

with the sum over all major fermentation products the gut bacteria release, FP_i, with $i = \{acetate, butyrate, formate, lactate, propionate, succinate\}$. e_i indicates the excretion of fermentation product i per bacterial biomass (**SI Text 2** above). We measured these numbers in pure cultures (**Figure 1**) and can estimate them for a complex microbiota by either considering the average across all 16 characterized strains or by weighing numbers according to relative species abundance (**SI Text 6** below). We can further simplify this formula and derive a total

excretion coefficient e_{tot}, which gives the following formulation for the total amount of excreted FP,

$$FP_{tot} = e_{tot} \cdot M_{feces,bact}$$

Section 3.2 Estimation via carbohydrates

The starting point for this estimation is the amount of carbohydrates which enters the large intestine and is available for bacteria digestion every day, M_{MACs}. This number can come from a direct characterization of luminal content or by estimating the diet-dependent mapping between consumed nutrients and those reaching the large intestine (see **SI Text 4** below). Assuming bacteria utilize all available carbohydrates for fermentative growth, the bacterial biomass produced per day follows as:

$$M_{bact} = M_{MACs}/\mathrm{u}$$

Here, u indicates the per biomass uptake of carbohydrates, a number which we again determined experimentally for the most abundant gut species (**Figure 1 and SI Text 2**). Similar to the estimation via feces, the total daily amount of fermentation products released to support the growth of this biomass follows as:

$$FP_{tot} = \sum_i FP_i = \sum_i e_i \cdot M_{bact}$$

with the sum over all major fermentation products the gut bacteria release $\{FP_i\}$. $i = \{acetate, butyrate, formate, lactate, propionate, succinate\}$ denotes again different fermentation products. e_i indicates the excretion of fermentation product i per bacterial biomass.

Section 3.3 Estimation via theoretical ATP yields (according to McNeil (24))

The estimation in the study by McNeil et al starts with fecal weight and bacterial content estimations. Specifically, McNeil et al use 15-20g of bacterial biomass lost via feces per day. Given published estimations of ATP yields they then derive that it requires approximately 1.5-2.0mol ATP per day to regenerate this biomass. With an estimation that the fermentation of 1mol hexose yields approximately 5mol ATP, one arrives at a number of 50-65g of carbohydrates per day that is needed for the gut microbiota in order to generate the lost biomass. By estimating the typical net synthesis of ATP resulting from the fermentation of one hexose they also estimate that fermentation of this amount of carbohydrates would yield 500-600mmol of short chain fatty acids, with a total energy value of 600-750kJ, representing 75% of the total energy in the carbohydrates, and 6-9% of the total energy requirements of the human host. This calculation via bacterial ATP requirements coupled to the ATP yield of anaerobic fermentation provides an additional point estimate for the total FP harvest as well as the energy contribution of the gut microbiota for the British reference case, complementing the estimates presented in **SI Text 3.1 and 3.2**.

Section 4: Mapping of nutrition data to microbiota-available carbohydrate

Nutritional data is typically reported as a breakdown of total carbohydrate, protein, fat, and dietary fiber, as well as the amount of sugar consumed by a person per time-period. We use data from the 1976 report on household food consumption and expenditure of the National Food Survey Committee in the United Kingdom (*3*) to estimate the microbiota-available carbohydrates for the

British reference scenario as follows. First, we assume all consumed sugar is absorbed in the small intestine, and thus lost to the microbiota. For glucose, uptake rates as high as 550mmol/h have been measured in humans (*25*, *26*), a number which is sufficient to explain the uptake of all glucose even in meals containing large amounts. Lower numbers of around 100mmol/h are reported for the hydrolysis and uptake of sucrose, the main sugar component in human nutrition (*27*) but these numbers are still very high compared to typical sugar consumption (e.g. about 59g or 172.4mmol sucrose per day for British reference diet). The situation might change in cases where most sugar is taken up in more poorly absorbable form such as fructose, where uptake rates are lower and transporters are easily saturated (*28*–*30*).

Second, we assume a constant fraction of the non-fiber, non-sugar carbohydrates to be available to the gut microbiota. This fraction of dietary carbohydrates mostly contains starches. Many starches can be enzymatically cleaved into glucose by human enzymes, which is taken up in the small intestine and constitutes an important source of calories for the human body. Even though the molecular components of starches are well-defined, starch breakdown is not. Different types of starch molecules are degraded at different speeds, depending on the folding and packaging of the macromolecule, water content, molecular structure, and temperature in complex ways (*31*, *32*). A fraction of the starches is completely inaccessible to host enzymes (the resistant starch fraction). The fraction of starches that pass through the small intestine into the large intestine has been reported to vary between 0% (pure soluble starch) and 96% (banana flour, (*31*)), with large variations, also depending on the type of food preparation (*33*–*35*). When considering staple foods, such as boiled potato and white bread, which account for most starch in the British reference diet, the numbers reported for the fraction of starch reaching the large intestine are 13% and 10% (*31*). For the analysis presented in the main text we assumed a fraction of 13% of total starch to be available to the microbiota. To further illustrate the possible variation of fermentation product release with starch availability, we further discuss the obtained distribution values of fermentation products for a lower and higher passage of starches (**Figures S4 and S8)**.

Third, we assume that a constant fraction of dietary fiber is accessible to the gut microbiota. In contrast to starches, almost all dietary fibers reach the gut microbiota. However, not all of it can be broken down by bacterial enzymes. This fraction can depend on the composition of the microbiota, as some fiber can only be broken down by highly specialized bacteria (*36*, *37*). For example, some common plant fibers such as cellulose and lignin are typically inaccessible to human gut microbiotas. They contribute to fecal bulk as non-bacterial mass and have a role in water retention in the colon, but do not contribute to bacterial fermentation. For our analysis, we assume a fraction of 50% of dietary fiber to be accessible to bacterial enzymes and thus serve as a nutrient source for the gut microbiota. In **Figures S4** and **S8**, we analyze how our results would change with lower (25%) and higher (75%) digestion fractions.

Importantly, fiber consumption can further impact bacterial fermentation via its strong effect on transit times. Given the high water-binding capacity of fiber, strong fiber consumption can substantially increase the bulk volume that passes the large intestine each day. Given a limited variability of the intestinal volume, fiber consumption thus leads to a strong increase in fecal wet weight and a strong decrease in transit time (*38*). This view is confirmed for example by a strong anticorrelation between transit time and fecal wet weight (**Figure S9D**). Importantly, for very high fiber consumption (and fecal wet weight), transit times can drop substantially below 24 hours. With 2-6 hours required for food to reach the large intestine, the biomass remains in the large

intestine for only a very limited amount of time. Particularly for harder to digest carbohydrates such short transit can severely reduce the efficiency with which bacteria digest carbohydrates. In our estimations, we do not explicitly model this dependence, but instead note that our analysis provides an upper boundary estimate, particularly for high fiber consumption (see also **Figure S9D**).

Section 5: Most released fermentation products are taken up by the host

To estimate the amount of fermentation products that the host obtains from growing bacteria, we need to estimate the fraction of fermentation products that are taken up by the host. As we outline in the main text, we estimate this fraction to be very high, and we therefore take the produced amount of fermentation products as a good (upper bound) estimate for the consumed fermentation products by the host. In the following, we discuss why this is justified. Besides consumption by the host, fermentation products might specifically be lost via feces (i) or consumed by cross-feeding microbes (ii). In addition, the turnover of fermentation products might also be shaped by the recycling of bacterial biomass (iii). In the following we discuss these three different possibilities separately.

i. Loss of fermentation products via feces is negligible. Concentrations of fermentation products in feces have been measured and the summed concentration of all major fermentation products rarely exceeds about 100mM (*39*). With an average fecal wet mass of 118 g/day for a Western diet (*2*), this corresponds to approximately 10 mmol of fermentation products which are secreted via feces each day. With the human gut microbiota releasing approx. 500 mmol of fermentation products each day (British reference scenario, **Figure 2**), 2% or less of the fermentation products leave the body via feces. Accordingly, most fermentation products remain in the host. These numbers also emphesize that measurements of FP in feces are a bad proxy for fermentation products released by the microbiota.
ii. Consumption of fermentation products by cross-feeding bacteria likely plays a minor role. Cross-feeding between members of the gut microbiota has been demonstrated in various studies (*19*, *40*–*43*), and cross-feeding is a way to optimize microbial energy retention from carbon sources. However, it does not allow gut bacteria to circumvent the fundamental constraint that, in anaerobic conditions, they have to produce fermentation products (**SI Text 1** above). Therefore, even if FPs are cross-fed between microbes, this typically leads to a change in the type of final FP, but not in the total amount. In addition, growth on low-quality nutrients such as FPs is likely very slow, leading to low abundance of strains pursuing this strategy in the face of bulk turnover in the large intestine (*44*). This view is well confirmed by metagenomics studies which show that the relative abundance of methanogens, sulfate-reducing bacteria, and other cross-feeders which carry metabolic genes to utilize fermentation products in anaerobic environments (*45*, *46*) remains very low, accounting for only a very tiny fraction of all bacterial biomass (*47*).
iii. Recycling of bacterial biomass does not substantially impact the harvest of fermentation product. Bacterial biomass contains sugars, proteins, and other potential nutrient sources. For these to become available for other bacteria, bacterial cell components would have to

leak into the gut lumen. This probably happens to some extent, triggered for example by lytic phages, but this effect is likely small and negligible when calculating the net turnover of biomass and fermentation products. We see this confirmed in our analysis, for example for the British reference diet, as the total bacterial mass lost each day is very close to the biomass that can be generated based on the amount of carbohydrates available to the microbiota.

Section 6: Estimate variation with microbiota composition

In the main text we described the variation of the daily fermentation product harvest with microbiome composition. As described in **SI Text 3** above, the daily release of different fermentation products FP_i , with $i \in$ {acetate, butyrate, format, lactate, propionate, succinate}, depends on the daily growth of bacterial mass $M_{bacteria}$ and the per biomass excretion of different fermentation products e_i required to enable this growth:

$$FP_i = e_i M_{bacteria}$$

We have measured the excretion of the different fermentation products of 16 highly abundant gut strains (**Figure 1** and **SI Text 2**). To estimate the variation of secretion across different microbiota samples we started with the relative abundance $\alpha_j^{species}$ of each species j which we experimentally characterized with a representative strain. To obtain these numbers for a large pool of microbiota samples from different studies we used specifically the abundance data provided by the curated metagenomics dataset (*48*). With these numbers, we can estimate the average excretion per biomass for each fermentation product i as

$$e_i = \sum_{j \in charaterized\ strains} e_{ij} \cdot \tilde{\alpha}_j^{species}$$

Here, e_{ij} denotes the measured excretion of fermentation product i per biomass of characterized strain j. $\tilde{\alpha}_j^{species}$is the abundance of strain j, normalized by the abundance of all measured strains, $\tilde{\alpha}_j^{species} = \alpha_j^{species} / \sum_j \alpha_j^{species}$. We similarly determined the uptake of carbohydrates per biomass as $u = \sum_j u_j \cdot \tilde{\alpha}_j^{species}$ to estimate the bacterial biomass $M_{bact} = M_{carb}/u$ from carbohydrates. Note that with this calculation, we assume that experimentally uncharacterized species present in a microbiota sample behave equally to the average of characterized species. This is a first reasonable assumption to illustrate the sample-to-sample variation of fermentation product release as the relative abundance of the sixteen characterized strains commonly accounts for a high fraction of overall bacterial biomass, on average 57% for a collection of microbiota samples from healthy individuals (see also **Figure S2A** for coverage numbers). However, in some samples the total abundance of characterized species is very low, with the characterized species accounting for even less than a few percent in a low fraction of the samples (**Figure S2B**, upper panel). To better estimate the average rates from the experimental data we thus also repeated the calculation on coarser taxonomic levels, assuming that the characterized species represent all species belonging to the same taxonomic group (TG). This approach is justified by the similarity in fermentation pathways among closely related species (**SI Text 1**). Specifically, we used the abundance data of detected species and their taxonomic classification to determine the fraction of biomass α_{TG}^{level} of all taxonomic groups which experimentally characterized strains represent for each of six specific taxonomic levels (phylum, class, order, family, genus, species). For

example, on the family level, eight taxonomic groups (families) are represented by the 16 characterized strains and we calculated their abundance by accounting for all the detected species belonging to each taxonomic group (e.g. $\alpha_{Bacteroidaceae}^{family}$ is typically the most abundant family when analyzing microbiota samples from healthy donors, see **Figure 3A**). With this abundance, we then calculated the average per biomass excretion and uptake similarly as before. For example, for the family level, we calculated

$$\epsilon_i^{family} = \sum_{TG \in represented\ families} \epsilon_{i,TG} \cdot \tilde{\alpha}_{TG}^{family}$$

With $\tilde{\alpha}_{TG}^{family} = \alpha_{TG}^{family} / \sum_j \alpha_{TG}^{family}$ denoting the renormalized abundance. $\epsilon_{i,TG}$ denotes the typical excretion for the specific taxonomic group which we calculated by averaging over all the excretion rates from experimentally characterized strains belonging to this taxonomic group. The advantage of these calculations on a coarser taxonomic level (e.g. family or class) is that the coverage of bacterial biomass becomes much higher. For example for the family level, on average a fraction of 87% percent of biomass is accounted for by this calculation when analyzing a collection of microbiota samples from healthy individuals, with the fraction being at least 70% in almost all the samples (**Figure 2B**, middle panel). However, we also introduce the additional assumption that experimentally characterized strains represent all species of the same taxonomic group. This assumption is justified based on similarities in reported metabolism (**SI Text 1**) but gets more problematic on higher taxonomic levels as species belonging to the same taxonomic group then come with a higher variety of metabolic strategies. As standard calculation we thus chose the family level as this level ensures a high coverage of biomass while still differentiating between metabolically diverse taxonomic groups of the Bacteroidota phylum, including the families Prevotellaceae and Bacteroidaceae which include Prevotella and Bacteroides species and which are known to differ in some aspects of their central metabolism (**SI Text 1**).

To analyze the variation of fermentation product with microbiota composition we performed the outlined calculations for each sample in different collections of microbiota samples. In the main text, we discuss the resulting variation in the daily FP production for microbiota samples from healthy donors (*22*, *23*)(**Figure 3**). Resulting variations in FP production for other studies and collections of microbiota samples can further be analyzed in the **Interactive Figure 1**. To illustrate how a specific taxonomic level in the calculations impacts the estimations we further show the analysis for healthy individuals using all taxonomic levels (**Figure S6**). All calculations to estimate the average per biomass uptake and excretion as well as the resulting daily FP production were performed with Python scripts which are available on the GitHub repository.

Section 7: Estimation of energy contribution

We estimate the energy content of the FPs released using their combustion enthalpies (*5*). The energy content of all fermentation products released each day follows from the release of each fermentation product and the corresponding enthalpy H_i listed in **Table S4**.

$$E_{ferm} = \sum_i H_i \cdot FP_i$$

Most of these fermentation products are taken up by the host (**SI Text 5**) where they are subsequently used in different parts of the body for respiration (*49*, *50*). To gain the relative contribution of this process to the total daily energy expenditure E_{exp} we calculate the ratio,

$$\alpha_{energy} = \frac{E_{ferm}}{E_{exp}}$$

For the British reference diet we used reported numbers, $E_{exp} \approx 2275\ kcal$ ($9.52\ MJ$) (*51*, *52*). To analyze the variation within the US population, we use the estimations from the NHANES study reported for each study participant (**Figure S7D** (*53*)). For the global variation analysis via fecal weight, we assumed values reported for the British reference diet, $E_{exp} \approx 2275\ kcal$ ($9.52\ MJ$). For the Hadza, we calculated values based on the consumed carbohydrates, fats, and proteins reported for each month, on average $E_{exp} \approx 2240\ kcal$ ($9.37\ MJ$).

Section 8: Mouse estimations

8.1 Estimation via feces

To estimate the contribution of the microbiota to energy homeostasis in mice we first followed a similar calculation as for humans using the via-feces estimation. We start with data for conventionally colonized mice fed ad libitum (*54*). The daily fecal dry mass these animals release is

$$M_{fec}^{mouse} = 0.82 \pm 0.09\ g/day$$

The variation here describes the SD of the reported variation in fecal weight. The microbial density in mouse feces lies within the range of 10^{11} and 10^{11} cells per milliliter (*55*, *56*). As we are not aware of more accurate measurements, we assume a similar fraction of the fecal dry matter to be bacteria as in humans (**Figure S4**), about 50%, leading to an excreted bacterial mass of

$$M_{feces,bac}^{mouse} \approx 0.41 g/day$$

As described above (**SI Text 3**), we calculate the amount of fermentation products as

$$FP_{tot}^{mouse} = \sum_i FP_i^{mouse} = \sum_i \epsilon_i M_{feces,bact}^{mouse} \approx 11.8 \pm 1.3\ mmol/day$$

As before (**SI Text 7**), this translates into an energy contribution of

$$E_{ferm}^{mouse} = \sum_i H_i \cdot FP_i \approx 10.6 \pm 1.2\ kJ/day$$

While variations remain, indirect calorimetry measurements consistently report a daily energy expenditure of $E_{exp}^{mouse} \approx 38{,}0\ kJ/day$ (*54*). With this, the bacterial contribution to energy homeostasis in mice is approximately,

$$\alpha_{energy}^{mouse} = \frac{E_{ferm}^{mouse}}{E_{exp}^{mouse}} \approx 28 \pm 3\%$$

To validate these results, we further use an alternative way to arrive at this number which is based on the comparison of germ-free and conventionally colonized mice.

8.2 Estimating microbial energy output by comparing energy retention in germ-free and colonized mice

As a second way of estimating the bacterial energy contribution in mice, we compare energy retention from food in conventionally colonized (CC) and germ-free (GF) mice, feeding ad libitum on chow. It is well known that food consumption is substantially higher in GF animals (*54*, *57*, *58*), which is consistent with a large bacterial contribution to energy homeostasis.

To estimate the energy fraction obtained from the microbiota, we start with the energy of daily consumed food determined in germ-free and conventional mice, as determined via calorimetry measurements (*54*):

$$H_{food}^{CC} = 54.5 \pm 8.5 \frac{kJ}{day}$$

$$H_{food}^{GF} = 62.7 \pm 8.9 \frac{kJ}{day}$$

Here and in the following, the provided ranges denote variations (SD) based on observed variations in food intake. In line with the hypothesis that GF mice cannot utilize dietary polysaccharides, the energy content of feces also varies.

$$H_{feces}^{CC} = 13.6 \pm 1.8\ kJ/day$$

$$H_{feces}^{GF} = 25.0 \pm 4.6\ kJ/day$$

Notable, the total energy mice extract from food each day, the difference between energy content in food and feces, is highly comparable between conventional and GF mice,

$$E_{extr}^{conv} = H_{food}^{CC} - H_{feces}^{CC} \approx 37.6\ kJ/day$$

$$E_{extr}^{GF} = H_{food}^{GF} - H_{feces}^{GF} \approx 40.9\ kJ/day$$

indicating that mice fed ad libitum adjust their food intake to match the energy they need independent of the source of this energy. With these numbers, we can calculate the efficiency of energy extraction from both colonization states:

$$\frac{E_{extr}^{CC}}{H_{food}^{CC}} \approx 75 \pm 12\%$$

$$\frac{E_{extr}^{GF}}{H_{food}^{GF}} \approx 60 \pm 9\%$$

This indicates a microbiota-derived energy gain in conventionally colonized mice of

$$\Delta E_{microbiota}^{mouse} = \left(\frac{E_{extr}^{CC}}{H_{food}^{CC}} - \frac{E_{extr}^{GF}}{H_{food}^{GF}} \right) \cdot H_{food}^{conv} \approx 8.1 \pm 1.8\ kJ/day$$

Accordingly, a fraction of

$$\alpha_{energy}^{mouse} = \Delta E_{microbiota}^{mouse} / E_{extr}^{CC} \approx 21 \pm 5\%$$

of the daily energy expenditure E_{extr} is supplied by the microbiota. This number is close to the estimation obtained via fecal microbial counts and the energy of fermentation products presented before ($28 \pm 3\%$).

8.3 Estimating relevant amounts of FPs in humans and mice

According to our estimates, colonized mice typically gain more of their daily energy need from FPs derived from their gut microbiota than humans (**Figure 6**). In absolute numbers, their FP harvest amounts to around 11.8mmol/day (fecal estimate, see **SI Text 8.1** above), which is roughly a factor 40 lower than what we calculated for humans (471mmol/day, fecal estimate, see **Figure 2A(iii)**). However, assuming a typical body weight of 30g for a mouse and 70kg for a human, the body weights of the two organisms differ by a factor of roughly 2300. Normalizing by weight thus yields a systemic FP harvest of approximately 393mmol/kg/day for mice, and 7mmol/kg/day for humans.

In addition to systemic effects such as behavioral modulation, FPs have been shown to have effects locally at the mucosal surface of the intestinal tract (*59*–*63*). The local FP harvest is different from the systemic one, because the relative large intestinal surface area is much greater in mice than in humans (0.03m^2/kg for a 70kg human (*64*), 2.3m^2/kg for a 30g mouse (*65*)). Taking into account this difference in surface areas, the per-area values we obtain for the FP harvest in mice and humans are much closer to each other (171 mmol/m^2/day for mice, and 233mmol/m^2/day for humans). This difference in relative large intestinal surface area suggests an evolutionary adaptation of uptake surface to the larger FP dependence in mice. Assuming that the dose dependence of mucosal immune modulation is comparable between mice and humans, the difference in the effect of SCFA between the two organisms is likely small in this respect.

References

1. E. Soupene, W. C. Van Heeswijk, J. Plumbridge, V. Stewart, D. Bertenthal, H. Lee, G. Prasad, O. Paliy, P. Charernnoppakul, S. Kustu, Physiological Studies of *Escherichia coli* Strain MG1655: Growth Defects and Apparent Cross-Regulation of Gene Expression. *J. Bacteriol.* **185**, 5611–5626 (2003).

2. J. B. Wyman, K. W. Heaton, A. P. Manning, A. C. Wicks, Variability of colonic function in healthy subjects. *Gut* **19**, 146–150 (1978).

3. *Household Food Consumption and Expenditure: Annual Report of the National Food Survey Committee* (H.M.S.O., ed. 1976) (1976).

4. A. M. Stephen, J. H. Cummings, The Microbial Contribution to Human Fecal Mass. *J. Med. Microbiol.* **13**, 45–56 (1980).

5. E. S. Domalski, E. D. Hearing, “Condensed Phase Heat Capacity Data” in *NIST Chemistry WebBook, NIST Standard Reference Database Number 69, Eds. P.J. Linstrom and W.G. Mallard* (National Institute of Standards and Technology, Gaithersburg MD, 20899, 2022; https://webbook.nist.gov) (2022).

6. R. K. Thauer, K. Jungermann, K. Decker, Energy conservation in chemotrophic anaerobic bacteria. *Bacteriol. Rev.* **41**, 100–180 (1977).

7. A. A. Salyers, Bacteroides of the human lower intestinal tract. *Annu. Rev. Microbiol.* **38**, 293–313 (1984).

8. V. H. Varel, M. P. Bryant, Nutritional Features of Bacteroides fragilis subsp. fragilis. *Appl. Microbiol.* **28** (1974).

9. N. Reichardt, S. H. Duncan, P. Young, A. Belenguer, C. M. Leitch, K. P. Scott, H. J. Flint, P. Louis, Phylogenetic distribution of three pathways for propionate production within the human gut microbiota. *ISME J.* **8**, 1323–1335 (2014).

10. P. Louis, H. J. Flint, Formation of propionate and butyrate by the human colonic microbiota. *Environ. Microbiol.* **19**, 29–41 (2017).

11. P. Louis, H. J. Flint, Diversity, metabolism and microbial ecology of butyrate-producing bacteria from the human large intestine. *FEMS Microbiol. Lett.* **294**, 1–8 (2009).

12. M. Vital, A. Karch, D. H. Pieper, Colonic Butyrate-Producing Communities in Humans: an Overview Using Omics Data. *mSystems* **2**, e00130-17 (2017).

13. G. T. Macfarlane, G. R. Gibson, “Carbohydrate Fermentation, Energy Transduction and Gas Metabolism in the Human Large Intestine” in *Gastrointestinal Microbiology* (vol. 134 of *Gastrointestinal Microbiology*, pp. 269–318 (1997).

14. M. A. Fischbach, J. L. Sonnenburg, Eating For Two: How Metabolism Establishes Interspecies Interactions in the Gut. *Cell Host Microbe* **10**, 336–347 (2011).

15. J. M. Macy, L. G. Ljungdahl, G. Gottschalk, Pathway of Succinate and Propionate Formation in Bacteroides fragilis. *J. Bacteriol.* **134**, 84–91 (1978).

16. T. Franke, U. Deppenmeier, Physiology and central carbon metabolism of the gut bacterium Prevotella copri. *Mol. Microbiol.* **109**, 528–540 (2018).

17. D. Caspari, J. M. Macy, The role of carbon dioxide in glucose metabolism of Bacteroides fragilis. *Arch. Microbiol.* **135**, 16–24 (1983).

18. P. Louis, P. Young, G. Holtrop, H. J. Flint, Diversity of human colonic butyrate-producing bacteria revealed by analysis of the butyryl-CoA:acetate CoA-transferase gene. *Environ. Microbiol.* **12**, 304–314 (2010).

19. A. Belenguer, S. H. Duncan, A. G. Calder, G. Holtrop, P. Louis, G. E. Lobley, H. J. Flint, Two Routes of Metabolic Cross-Feeding between Bifidobacterium adolescentis and Butyrate-Producing Anaerobes from the Human Gut. *Appl. Environ. Microbiol.* **72**, 3593–3599 (2006).

20. A. Bezkorovainy, R. Miller-Catchpole, *Biochemistry and Physiology of Bifidobacteria* (CRC Press, ed. 1) (2020).

21. F. C. Neidhardt, J. L. Ingraham, M. Schaechter, *Physiology of the Bacterial Cell - A Molecular Approach* (Sinauer Associates, Sunderland, MA, USA) (1990).

22. J. Lloyd-Price, C. Arze, A. N. Ananthakrishnan, M. Schirmer, J. Avila-Pacheco, T. W. Poon, E. Andrews, N. J. Ajami, K. S. Bonham, C. J. Brislawn, D. Casero, H. Courtney, A. Gonzalez, T. G. Graeber, A. B. Hall, K. Lake, C. J. Landers, H. Mallick, D. R. Plichta, M. Prasad, G. Rahnavard, J. Sauk, D. Shungin, Y. Vázquez-Baeza, R. A. White, J. Braun, L. A. Denson, J. K. Jansson, R. Knight, S. Kugathasan, D. P. B. McGovern, J. F. Petrosino, T. S. Stappenbeck, H. S. Winter, C. B. Clish, E. A. Franzosa, H. Vlamakis, R. J. Xavier, C. Huttenhower, Multi-omics of the gut microbial ecosystem in inflammatory bowel diseases. *Nature* **569**, 655–662 (2019).

23. M. Schirmer, E. A. Franzosa, J. Lloyd-Price, L. J. McIver, R. Schwager, T. W. Poon, A. N. Ananthakrishnan, E. Andrews, G. Barron, K. Lake, M. Prasad, J. Sauk, B. Stevens, R. G. Wilson, J. Braun, L. A. Denson, S. Kugathasan, D. P. B. McGovern, H. Vlamakis, R. J. Xavier, C. Huttenhower, Dynamics of metatranscription in the inflammatory bowel disease gut microbiome. *Nat. Microbiol.* **3**, 337–346 (2018).

24. N. I. McNeil, The contribution of the large intestine to energy supplies in man. *Am. J. Clin. Nutr.* **39**, 338–342 (1984).

25. A. R. Coggan, E. F. Coyle, Effect of carbohydrate feedings during high-intensity exercise. *J. Appl. Physiol.* **65**, 1703–1709 (1988).

26. M. Hargreaves, C. A. Briggs, Effect of carbohydrate ingestion on exercise metabolism. *J. Appl. Physiol.* **65**, 1553–1555 (1988).

27. G. M. Gray, F. J. Ingelfinger, Intestinal absorption of sucrose in man: interrelation of hydrolysis and monosaccharide product absorption. *J. Clin. Invest.* **45**, 388–398 (1966).

28. P. R. Gibson, E. Newnham, J. S. Barrett, S. J. Shepherd, J. G. Muir, Review article: fructose malabsorption and the bigger picture. *Aliment. Pharmacol. Ther.* **25**, 349–363 (2007).

29. P. L. Beyer, E. M. Caviar, R. W. McCallum, Fructose Intake at Current Levels in the United States May Cause Gastrointestinal Distress in Normal Adults. *J. Am. Diet. Assoc.* **105**, 1559–1566 (2005).

30. Y. K. Choi, F. C. Johlin, R. W. Summers, M. Jackson, S. S. C. Rao, Fructose Intolerance: An Under-Recognized Problem. *Am. J. Gastroenterol.* **98**, 1348–1353 (2003).

31. H. N. Englyst, S. M. Kingman, J. H. Cummings, Classification and measurement of nutritionally important starch fractions. *Eur. J. Clin. Nutr.* **46 Suppl 2**, S33-50 (1992).

32. K. N. Englyst, S. Liu, H. N. Englyst, Nutritional characterization and measurement of dietary carbohydrates. *Eur. J. Clin. Nutr.* **61**, S19–S39 (2007).

33. H. N. Englyst, J. H. Cummings, Digestion of the polysaccharides of some cereal foods in the human small intestine. *Am. J. Clin. Nutr.* **42**, 778–787 (1985).

34. H. N. Englyst, J. H. Cummings, Digestion of the carbohydrates of banana (Musa paradisiaca sapientum) in the human small intestine. *Am. J. Clin. Nutr.* **44**, 42–50 (1986).

35. H. N. Englyst, J. H. Cummings, Digestion of polysaccharides of potato in the small intestine of man. *Am. J. Clin. Nutr.* **45**, 423–431 (1987).

36. J.-H. Hehemann, A. G. Kelly, N. A. Pudlo, E. C. Martens, A. B. Boraston, Bacteria of the human gut microbiome catabolize red seaweed glycans with carbohydrate-active enzyme updates from extrinsic microbes. *Proc. Natl. Acad. Sci. U. S. A.* **109**, 19786–19791 (2012).

37. E. S. Shepherd, W. C. DeLoache, K. M. Pruss, W. R. Whitaker, J. L. Sonnenburg, An exclusive metabolic niche enables strain engraftment in the gut microbiota. *Nature* **557**, 434–438 (2018).

38. A. M. Stephen, J. H. Cummings, Mechanism of action of dietary fibre in the human colon. *Nature* **284**, 283–284 (1980).

39. T. Høverstad, O. Fausa, A. Bjørneklett, T. Bøhmer, Short-Chain Fatty Acids in the Normal Human Feces. *Scand. J. Gastroenterol.* **19**, 375–381 (1984).

40. L. D. Vuyst, F. Leroy, Cross-feeding between bifidobacteria and butyrate-producing colon bacteria explains bifdobacterial competitiveness, butyrate production, and gas production. *Int. J. Food Microbiol.* **149**, 73–80 (2011).

41. E. H. Crost, G. Le Gall, J. A. Laverde-Gomez, I. Mukhopadhya, H. J. Flint, N. Juge, Mechanistic Insights Into the Cross-Feeding of Ruminococcus gnavus and Ruminococcus bromii on Host and Dietary Carbohydrates. *Front. Microbiol.* **9**, 2558 (2018).

42. E. C. Soto-Martin, I. Warnke, F. M. Farquharson, M. Christodoulou, G. Horgan, M. Derrien, J.-M. Faurie, H. J. Flint, S. H. Duncan, P. Louis, Vitamin Biosynthesis by Human Gut Butyrate-Producing Bacteria and Cross-Feeding in Synthetic Microbial Communities. *mBio* **11**, e00886-20 (2020).

43. P. Pérez Escriva, T. Fuhrer, U. Sauer, Distinct N and C Cross-Feeding Networks in a Synthetic Mouse Gut Consortium. *mSystems* **7**, e01484-21 (2022).

44. J. Cremer, I. Segota, C. Yang, M. Arnoldini, J. T. Sauls, Z. Zhang, E. Gutierrez, A. Groisman, T. Hwa, Effect of flow and peristaltic mixing on bacterial growth in a gut-like channel. *Proc. Natl. Acad. Sci. U. S. A.* **113**, 11414–11419 (2016).

45. G. R. Gibson, J. H. Cummings, G. T. Macfarlane, C. Allison, I. Segal, H. H. Vorster, A. R. Walker, Alternative pathways for hydrogen disposal during fermentation in the human colon. *Gut* **31**, 679–683 (1990).

46. G. R. Gibson, G. T. Macfarlane, J. H. Cummings, Sulphate reducing bacteria and hydrogen metabolism in the human large intestine. *Gut* **34**, 437–439 (1993).

47. The Integrative HMP (iHMP) Research Network Consortium, The Integrative Human Microbiome Project. *Nature* **569**, 641–648 (2019).

48. E. Pasolli, L. Schiffer, P. Manghi, A. Renson, V. Obenchain, D. T. Truong, F. Beghini, F. Malik, M. Ramos, J. B. Dowd, C. Huttenhower, M. Morgan, N. Segata, L. Waldron, Accessible, curated metagenomic data through ExperimentHub. *Nat. Methods* **14**, 1023–1024 (2017).

49. G. den Besten, K. Lange, R. Havinga, T. H. van Dijk, A. Gerding, K. van Eunen, M. Müller, A. K. Groen, G. J. Hooiveld, B. M. Bakker, D.-J. Reijngoud, Gut-derived short-chain fatty acids are vividly assimilated into host carbohydrates and lipids. *Am. J. Physiol.-Gastrointest. Liver Physiol.* **305**, G900–G910 (2013).

50. G. den Besten, K. van Eunen, A. K. Groen, K. Venema, D.-J. Reijngoud, B. M. Bakker, The role of short-chain fatty acids in the interplay between diet, gut microbiota, and host energy metabolism. *J. Lipid Res.* **54**, 2325–2340 (2013).

51. FAO, Human energy requirements. Report of a Joint FAO/WHO/UNU Expert Consultation (2001).

52. H. Pontzer, D. A. Raichlen, B. M. Wood, M. Emery Thompson, S. B. Racette, A. Z. P. Mabulla, F. W. Marlowe, Energy expenditure and activity among Hadza hunter-gatherers. *Am. J. Hum. Biol.* **27**, 628–637 (2015).

53. *National Health and Nutrition Examination Survey (NHANES) Data 2017-2018* (Centers for Disease Control and Prevention (CDC). National Center for Health Statistics (NCHS), Hyattsville, MD: US Department of Health and Human Services) (2018).

54. D. Hoces, J. Lan, W. Sun, T. Geiser, M. L. Stäubli, E. Cappio Barazzone, M. Arnoldini, T. D. Challa, M. Klug, A. Kellenberger, S. Nowok, E. Faccin, A. J. Macpherson, B. Stecher, S. Sunagawa, R. Zenobi, W.-D. Hardt, C. Wolfrum, E. Slack, Metabolic reconstitution of germ-free mice by a gnotobiotic microbiota varies over the circadian cycle. *PLOS Biol.* **20**, e3001743 (2022).

55. J. T. Barlow, S. R. Bogatyrev, R. F. Ismagilov, A quantitative sequencing framework for absolute abundance measurements of mucosal and lumenal microbial communities. *Nat. Commun.* **11**, 2590 (2020).

56. D. Vandeputte, G. Kathagen, K. D'hoe, S. Vieira-Silva, M. Valles-Colomer, J. Sabino, J. Wang, R. Y. Tito, L. D. Commer, Y. Darzi, S. Vermeire, G. Falony, J. Raes, Quantitative microbiome profiling links gut community variation to microbial load. *Nature* **551**, 507–511 (2017).

57. F. Bäckhed, H. Ding, T. Wang, L. V. Hooper, G. Y. Koh, A. Nagy, C. F. Semenkovich, J. I. Gordon, The gut microbiota as an environmental factor that regulates fat storage. *Proc. Natl. Acad. Sci. U. S. A.* **101**, 15718–15723 (2004).

58. B. S. Wostmann, C. Larkin, A. Moriarty, E. Bruckner-Kardoss, Dietary Intake, Energy Metabolism, and Excretory Losses of Adult Male Germfree Wistar Rats. *Lab. Anim. Sci.* **33**, 3 (1983).

59. W. Wu, M. Sun, F. Chen, A. T. Cao, H. Liu, Y. Zhao, X. Huang, Y. Xiao, S. Yao, Q. Zhao, Z. Liu, Y. Cong, Microbiota metabolite short-chain fatty acid acetate promotes intestinal IgA response to microbiota which is mediated by GPR43. *Mucosal Immunol.* **10**, 946–956 (2017).

60. M. Kim, Y. Qie, J. Park, C. H. Kim, Gut Microbial Metabolites Fuel Host Antibody Responses. *Cell Host Microbe* **20**, 202–214 (2016).

61. T. Takeuchi, E. Miyauchi, T. Kanaya, T. Kato, Y. Nakanishi, T. Watanabe, T. Kitami, T. Taida, T. Sasaki, H. Negishi, S. Shimamoto, A. Matsuyama, I. Kimura, I. R. Williams, O. Ohara, H. Ohno, Acetate differentially regulates IgA reactivity to commensal bacteria. *Nature* **595**, 560–564 (2021).

62. Y. Furusawa, Y. Obata, S. Fukuda, T. A. Endo, G. Nakato, D. Takahashi, Y. Nakanishi, C. Uetake, K. Kato, T. Kato, M. Takahashi, N. N. Fukuda, S. Murakami, E. Miyauchi, S. Hino, K. Atarashi, S. Onawa, Y. Fujimura, T. Lockett, J. M. Clarke, D. L. Topping, M. Tomita, S. Hori, O. Ohara, T. Morita, H. Koseki, J. Kikuchi, K. Honda, K. Hase, H. Ohno, Commensal microbe-derived butyrate induces the differentiation of colonic regulatory T cells. *Nature*, 1–8 (2013).

63. N. Singh, A. Gurav, S. Sivaprakasam, E. Brady, R. Padia, H. Shi, M. Thangaraju, P. D. Prasad, S. Manicassamy, D. H. Munn, J. R. Lee, S. Offermanns, V. Ganapathy, Activation of Gpr109a, Receptor for Niacin and the Commensal Metabolite Butyrate, Suppresses Colonic Inflammation and Carcinogenesis. *Immunity* **40**, 128–139 (2014).

64. H. F. Helander, L. Fändriks, Surface area of the digestive tract – revisited. *Scand. J. Gastroenterol.* **49**, 681–689 (2014).

65. C. Casteleyn, A. Rekecki, A. V. D. Aa, P. Simoens, W. V. D. Broeck, Surface area assessment of the murine intestinal tract as a prerequisite for oral dose translation from mouse to man. *Lab. Anim.* **44**, 176–183 (2010).